



Short communication

## Active lithium replenishment to extend the life of a cell employing carbon and iron phosphate electrodes

John Wang<sup>a,\*</sup>, Souren Soukiazian<sup>a</sup>, Mark Verbrugge<sup>b</sup>, Harshad Tataria<sup>c</sup>, Dwaine Coates<sup>d</sup>, David Hall<sup>e</sup>, Ping Liu<sup>a</sup>

<sup>a</sup> HRL Laboratories, LLC, Malibu, CA, United States

<sup>b</sup> GM, Chemical Sciences and Materials Systems Lab, United States

<sup>c</sup> GM, Global Battery Systems Engineering, Global Vehicle Engineering, United States

<sup>d</sup> Boeing, Huntington Beach, CA, United States

<sup>e</sup> Boeing, Huntsville, AL, United States

### ARTICLE INFO

#### Article history:

Received 8 January 2011

Received in revised form 23 February 2011

Accepted 24 February 2011

Available online 6 March 2011

#### Keywords:

LiFePO<sub>4</sub> battery

Lithium replenishment

Battery life

LiFePO<sub>4</sub>/graphite

Cycle life

### ABSTRACT

We describe and implement a method of extending the life of a LiFePO<sub>4</sub>/graphite lithium ion battery by replenishing the lost active lithium during cell operation and concomitant capacity fade. The approach may prove helpful in terms of increasing lithium ion cell life. After the cell had lost 30% of its capacity, analysis showed that the cell had not experienced significant impedance increase or cathode capacity loss, and the anode had lost about 5% of its storage capacity. The analysis confirmed that the loss of active lithium greatly outpaced the loss of capacity for either electrode and is responsible for cell capacity decay. The cathode was then discharged against an external lithium electrode to increase the amount of active lithium within the cell. About half of the lost capacity was recovered, and the cell cycled for 1500 more cycles. Active lithium replenishment from a reserve electrode may be an effective method of extending the life of lithium ion batteries.

© 2011 Elsevier B.V. All rights reserved.

### 1. Introduction

The main objective of this work is to provide a practical approach to significantly increase the life of lithium ion batteries. These batteries are being considered for applications that demand exceptionally long calendar and cycle lives. Examples are hybrid, plug-in, and pure electric vehicles, as well as satellites and other aerospace applications. Common methods of extending battery life include the employment of long life cathode (positive electrode) and anode (negative electrode) materials and the restriction of battery operation to avoid conditions detrimental to battery life. Examples of conditions to avoid include high and low temperatures, high depths of discharge, and high rates [1–5]. These restrictions invariably lead to under-utilization of the battery relative to nominal specifications, thus lowering effective energy density of the battery. In addition, precise control of cell temperature with aggressive thermal management on the pack level is often required, which adds significantly to system weight, volume, and cost. Even with these

operation and design restrictions, lithium ion battery life is still limited to at most a few thousand deep-discharge cycles.

The mechanisms of performance decay for lithium ion batteries have been subjects of extensive studies [1,6–30]. In general, batteries lose capacity and/or power capability due to resistance increase [7–9,14,31,32]. Capacity loss of a battery is related to active material loss. The three important quantities to consider are the storage capacity of the cathode, that of the anode, and the amount of the active lithium cycling between the two electrodes. When a conventional lithium ion battery is fabricated, the (carbon) anode capacity is always larger than that of the cathode. This design is necessary to prevent the possibility of lithium metal plating during charging if active lithium exceeds the capacity of the negative electrode. The cathode initially holds all the active lithium prior to the first charge. A portion of the active lithium is consumed to form the solid state interface layer during the first charge (also known as the formation cycle). Consequently, the amount of active lithium is smaller than the positive electrode capacity. It is obvious that the amount of active lithium is smaller than the storage capacity of either of the two electrodes. This amount is equivalent to the measured cell capacity at very low rates. When the amount of active lithium is reduced during a battery's calendar and cycle life, the cell capacity decreases accordingly. At the same time, the storage capacities of the electrodes can also decrease. However, as long as the amount

\* Corresponding author at: HRL Laboratories, LLC, Energy Technologies Dept., 3011 Malibu Canyon Rd., Malibu, CA, United States. Tel.: +1 310 317 5155; fax: +1 310 317 5840.

E-mail address: [jswang@hrl.com](mailto:jswang@hrl.com) (J. Wang).

of active lithium remains smaller than the storage capacity of both electrodes, the cell capacity will always correspond to the amount of active lithium.

In this work, we employ a lithium replenishment technique to increase the amount of active lithium in a cycled battery cell to restore part of its lost capacity and extend its cycle life. This technique uses a lithium storage electrode that is not active during battery operation but can be discharged against either the cathode or the anode when there is a need to increase active lithium amount. We carried out the lithium replenishment using a lithium ion battery with a  $\text{LiFePO}_4$  positive and a graphite negative electrode. This battery is a promising candidate for high power applications such as for use in hybrid electric vehicles (HEVs) and power tools because of high thermal stability, potentially low cost, and good cycle life [33–40]. First, a  $\text{LiFePO}_4$ /graphite commercial cell was cycled to induce capacity fade. After the cell has lost a significant amount of its capacity, active lithium was inserted into the battery by discharging the positive electrode against an external lithium source (corresponding to lithium insertion of the cathode). We find that a significant amount of the lost capacity is recovered, and we examine the resultant cycling performance of the replenished cell.

## 2. Experimental

The commercially available 2.2 Ah, 26,650 cylindrical cells were purchased from A123Systems Inc. The cell chemistries involve a  $\text{LiFePO}_4$  positive electrode and a graphitic carbon negative electrode. The battery was cycled at 45 °C to induce capacity fade. The cycling test was performed on an Arbin BT-2400 system (Arbin Instruments, TX). During each cycle, the cell was charged to a maximum voltage of 3.6 V at a  $C/2$  rate and a voltage hold was applied until the current was less than  $C/20$ , or 0.1 A. 80% Depth-of-Discharge (DOD) or a capacity of 1.6 Ah at a rate of  $C/2$  was used for the discharge cycle. End of discharge voltage of 2.0 V was used as a cut-off voltage indicating the cell has reached the end of life (EOL).

Prior to the cycling test, the cell capacity was characterized by constant current charge/discharge measurements at rates of 6C,  $C/2$ , and  $C/20$ . At each rate, two cycles were measured and the results from the second cycle were recorded. During the cycling test, the cell was stopped periodically for additional capacity characterization.

Lithium replenishment procedures were carried out after the cell reached the End-of-Life (EOL). Fig. 1 shows the setup for the lithium replenishment experiments. All the procedures were performed in an argon filled glove box. An EOL cell was opened at the bottom and immersed into an electrolyte solution of 1 M  $\text{LiPF}_6$  in EC/DMC (1:1). A lithium electrode was placed in the electrolyte to serve as the lithium source for replenishment. The positive electrode of the cell was discharged against the lithium metal electrode at a constant current of 0.5 mA while the graphite anode was idling. The cell was allowed to rest for 24 h, and the capacity was measured between the cathode and the graphite anode while the lithium served as a reference electrode.

## 3. Results and discussion

Our previous work has established that the aging mechanism of the  $\text{LiFePO}_4$ /graphite batteries is dominated by cell capacity loss during cycling due to the loss of active lithium under moderate operating conditions as would be expected in many applications [5]. Using detailed electrochemical analysis combined with destructive physical analysis, we have determined the capacity fading behaviors of all three major components of a battery. Key results derived include: (1)  $\text{LiFePO}_4$  cathode was very robust upon cycling

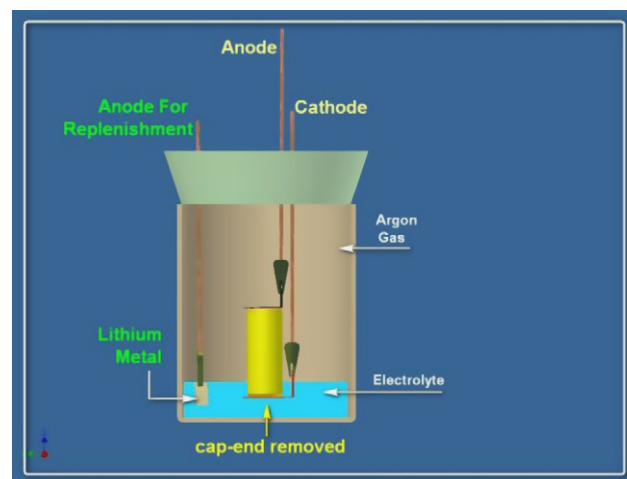


Fig. 1. Schematic of an experimental setup for lithium replenishment. A cylindrical cell with its end cap open is immersed in an electrolyte solution. A lithium metal electrode is used to provide active lithium to one of the two electrodes during replenishment.

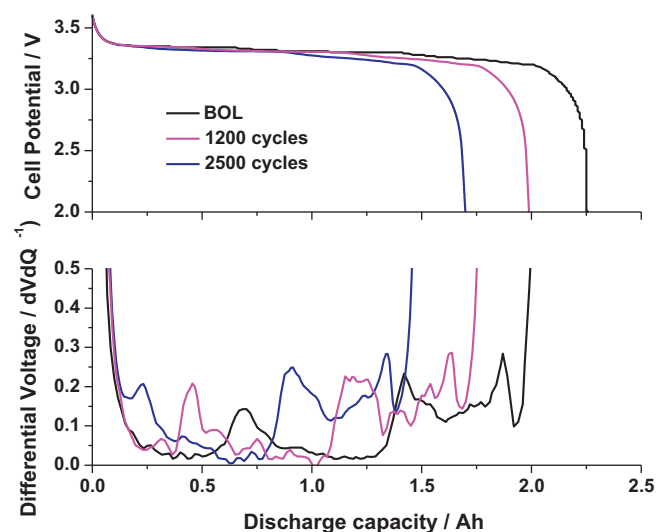


Fig. 2. (Top) Evolution of discharge profiles for a  $\text{LiFePO}_4$ /graphite lithium ion cell after cycling tests at 80% DOD,  $C/2$  rate, and 45 °C; (bottom) differentiation curves of the discharge profiles.

with negligible capacity loss; (2) small capacity loss was observed on graphite anode; and most importantly, (3) the loss of active lithium outpaced the loss of graphite electrode and cell capacity was limited by the amount of active lithium. In other words, the active storage capacities for both the positive electrode and the negative electrode are always higher than the amount of active lithium and both electrodes become increasingly under-utilized. In this report, we first confirm whether this battery cell follows the same loss mechanism by analyzing the evolution of the charge–discharge profiles during cycling.

The beginning of life capacity of the cell was 2.237 Ah. The cycle test conditions correspond to 80% DOD (depth of discharge), 45 °C, and  $C/2$  rate. Periodically, cell capacities were measured to monitor decay; the discharge curves are shown in Fig. 2. Consistent with our previous observations, the cell does not appear to experience appreciable resistance increase since the discharge voltage remains constant. Rather, the cell capacity gradually decreases. After 2730 cycles, the cell has lost 30% of its initial capacity. The capacity eventually fell to 1.514 Ah, which we define as the end of life for the cell.

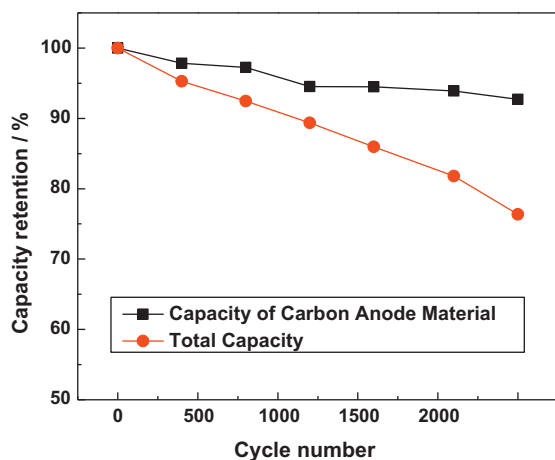


Fig. 3. Capacity retention of the cell and the carbon anode material as a function of cycle number. The capacity of the carbon anode material was deduced from analysis of the differentiation curves shown in Fig. 2.

We next analyze the discharge curves to quantify the loss of active material during cycling. The  $dV/dQ$  technique has been described previously [5,41–43]. ( $V$  denotes voltage and  $Q$  represents Coulombic capacity.) In short, the discharge curves of the cell carry the features from the graphite electrode, since the  $\text{LiFePO}_4$  cathode does not contribute substantially to any of the  $V$ - $Q$  features. In the  $dV/dQ$  vs  $Q$  curve, the peaks correspond to specific lithium concentrations in graphite; i.e.,  $x$  in  $\text{Li}_x\text{C}_6$ . The distance between the peaks, in terms of capacity, is proportional to the amount of graphite. If there is a loss of graphite, this distance will decrease. If there is a loss of active lithium, the peaks will move an equivalent amount, in terms of capacity, towards lower state of discharge, since the lithium concentration in graphite will decrease at the beginning of discharge. By taking into account these two factors and the employment of discharge profiles of individual electrodes vs  $\text{Li}$ , we are able to simulate the cell discharge profile from individual electrode data and deduce the remaining capacities of individual electrodes. Fig. 3 summarizes the results for this cell. While the cell has lost ~30% of its capacity or active lithium, the graphite anode lost about 10% of its storage capacity, and the  $\text{LiFePO}_4$  cathode suffered no measurable capacity loss.

Since the loss of active lithium greatly outpaced the loss of graphite anode, it is possible to recover part of the lost capacity by replenishing active lithium as long as the total lithium in the cell does not exceed the capacity of either electrode. After the battery has reached the EOL, cell capacity was then replenished by discharging the cathode against a lithium metal electrode as shown in Fig. 1. The battery was then left at open circuit for 24 h to equilibrate the electrodes. Fig. 4 shows the  $C/2$  discharge curves after each period of lithium replenishment. We started with an EOL cell with a capacity of 1.514 Ah. After 6 periods of lithium replenishment processes, the cell capacity has increased to 1.915 Ah. Hence, 0.4 Ah of active lithium was inserted into the battery. The discharge curves after each period of lithium replenishment are very similar to those before replenishment of lithium. The results of the lithium replenishment are also summarized in Table 1. Note that the charge consumed for lithium replenishment is much greater than the observed increase in active lithium. In other words, the coulomb efficiency of the process is only around 50%. The reason for this low efficiency is not yet known but likely related to parasitic reactions in the system. A possible source is the battery casing material that is immersed in the electrolyte and could consume charge due to surface reactions. During each capacity characterization, we also monitor the anode voltage vs lithium metal, which serves as a reference electrode. Fig. 5 shows both the cell voltage

Table 1

Summary of cell capacity rejuvenation after each period of lithium replenishment.

| Period | Lithium inserted (mAh) | Cell capacity rejuvenated (mAh) |
|--------|------------------------|---------------------------------|
| P1     | 50                     | 37                              |
| P2     | 50                     | 31                              |
| P3     | 80                     | 47                              |
| P4     | 150                    | 74                              |
| P5     | 200                    | 95                              |
| P6     | 200                    | 116                             |
| Totals | 630                    | 400                             |

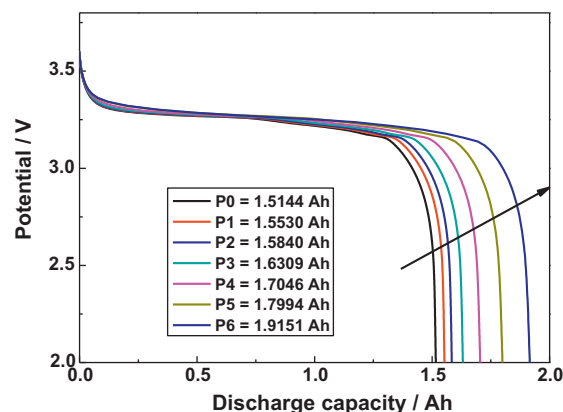


Fig. 4. Discharge curves of the  $\text{LiFePO}_4$  battery after each period of lithium replenishment; the replenishment is performed by discharging the cathode against a lithium metal electrode.

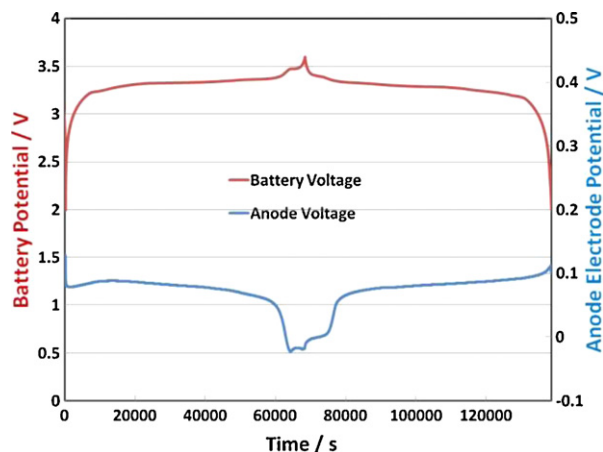


Fig. 5. Battery voltage and anode voltage curves after period 6 of lithium replenishment, recorded at a  $C/20$  rate.

and anode voltage after period 6 of the lithium replenishment. The anode potential relaxed to  $\sim 0\text{V}$  vs  $\text{Li}$  indicating that lithium plating has occurred at the anode, indicating that the active lithium amount in the system exceeded the capacity of the negative electrode. Therefore, we terminated the lithium replenishment process after period 6 for a total of 0.4 Ah of lithium insertion.

While these experiments demonstrate that we are able to insert active lithium into an EOL battery to increase its capacity, it is of great importance to investigate the cycling performance of the rejuvenated battery. We cycled the cell at 80% DOD,  $C/2$  rate, and room temperature. Fig. 6 shows the evolution of the cell discharge profiles which are very similar to those prior to lithium replenishment and show no signs of significant resistance increase. The cell successfully performed 1500 additional cycles, after which its capacity was 1.62 Ah.

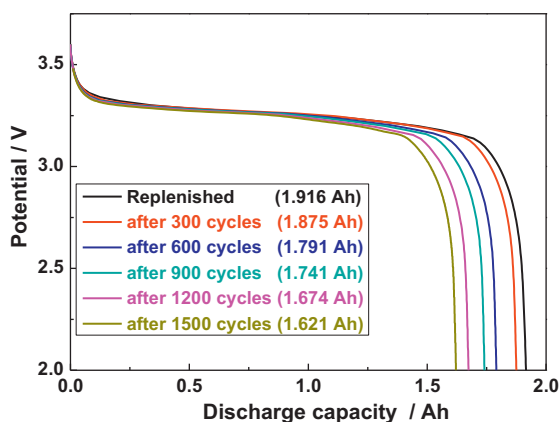


Fig. 6. Evolution of cell discharge curves after lithium replenishment. 1500 additional cycles are demonstrated.

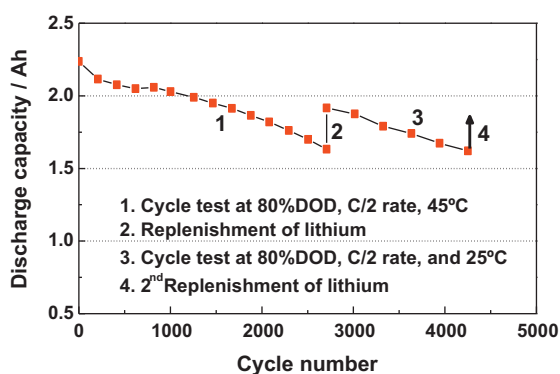


Fig. 7. Capacity fade profiles of the cell recorded before and after lithium replenishment. Before the lithium replenishment, the cycle test conditions were at 80% DOD, 45 °C, and C/2 rate; after the lithium replenishment the cycle test conditions were at 80% DOD, 25 °C, and C/2 rate.

#### 4. Summary and conclusions

This work demonstrates that active lithium can be inserted into a degraded lithium ion cell to extend its cycle life. More than 50% (0.4 Ah) of the lost capacity of an EOL  $\text{LiFePO}_4/\text{graphite}$  cell was recovered and the cell was then subjected to 1500 additional cycles (Fig. 7). The concept is most efficient when a lithium battery experiences little resistance rise and loses its capacity due to a reduction in active lithium. In the case of a  $\text{LiFePO}_4/\text{graphite}$  cell, the loss of active lithium greatly outpaces the capacity loss of either electrode under moderate cycling conditions consistent with most cell applications. By replenishing the active lithium from a reserve lithium storage material, the capacity of the battery can be partially recovered. Our results suggest novel designs for lithium ion batteries where a third electrode is built in to act as an active lithium reserve, which will provide active lithium on demand. A major advantage of this approach is that the reserve electrode adds very little additional weight or volume to the battery, since lithium metal or other high capacity materials can be used that do not need to be repeatedly cycled.

While this work shows promise for the in situ rejuvenation of a lithium ion battery, there are many integration issues and associated open questions. For example, the current demonstration

employs a very low current to perform the lithium replenishment due to the tight wound jelly roll design of the cylindrical cell. Further development in engineering design of the battery is necessary to significantly increase the rate of lithium replenishment to enable its use in practical systems.

#### References

- [1] D.P. Abraham, E.M. Reynolds, P.L. Schultz, A.N. Jansen, D.W. Dees, *J. Electrochem. Soc.* 153 (2006) A1610.
- [2] K. Amine, J. Liu, I. Belharouak, *Electrochem. Commun.* 7 (2005) 669.
- [3] M. Armand, J.M. Tarascon, *Nature* 451 (2008) 652.
- [4] K.Y. Chung, H.S. Lee, W.S. Yoon, J. McBreen, X.Q. Yang, *J. Electrochem. Soc.* 153 (2006) A774.
- [5] P. Liu, J. Wang, J. Hicks-Garner, E. Sherman, S. Soukiazian, M.W. Verbrugge, H. Tataria, J. Musser, P. Finamore, *J. Electrochem. Soc.* 157 (2010) A499.
- [6] M. Balasubramanian, H.S. Lee, X. Sun, X.Q. Yang, A.R. Moodenbaugh, J. McBreen, D.A. Fischer, Z. Fu, *Electrochem. Solid-State Lett.* 5 (2002) A22.
- [7] I. Bloom, S.A. Jones, E.G. Polzin, V.S. Battaglia, G.L. Henriksen, C.G. Motloch, R.B. Wright, R.G. Jungst, H.L. Case, D.H. Doughty, *J. Power Sources* 111 (2002) 152.
- [8] M. Broussely, S. Herreyre, P. Biensan, P. Kaszlejna, K. Nechev, R.J. Staniewicz, *J. Power Sources* 97–98 (2001) 13.
- [9] J. Christensen, J. Newman, *J. Electrochem. Soc.* 150 (2003) A1416.
- [10] J. Christensen, J. Newman, *J. Electrochem. Soc.* 151 (2004) A1977.
- [11] J. Christensen, J. Newman, *J. Electrochem. Soc.* 152 (2005) A818.
- [12] M. Dubarry, B.Y. Liaw, *J. Power Sources* 174 (2007) 856.
- [13] M. Dubarry, B.Y. Liaw, *J. Power Sources* 194 (2009) 541.
- [14] B.Y. Liaw, R.G. Jungst, G. Nagasubramanian, H.L. Case, D.H. Doughty, *J. Power Sources* 140 (2005) 157.
- [15] G. Ning, R.E. White, B.N. Popov, *Electrochim. Acta* 51 (2006) 2012.
- [16] P. Ramadass, B. Haran, P.M. Gomadam, R. White, B.N. Popov, *J. Electrochem. Soc.* 151 (2004) A196.
- [17] R.P. Ramasamy, J.W. Lee, B.N. Popov, *J. Power Sources* 166 (2007) 266.
- [18] R.B. Wright, C.G. Motloch, J.R. Belt, J.P. Christophersen, C.D. Ho, R.A. Richardson, I. Bloom, S.A. Jones, V.S. Battaglia, G.L. Henriksen, T. Unkelhaeuser, D. Ingersoll, H.L. Case, S.A. Rogers, R.A. Sutula, *J. Power Sources* 110 (2002) 445.
- [19] T. Yoshida, M. Takahashi, S. Morikawa, C. Ihara, H. Katsukawa, T. Shiratsuchi, J. Yamaki, *J. Electrochem. Soc.* 153 (2006) A576.
- [20] H. Ploehn, P. Ramadass, R. White, *J. Electrochem. Soc.* 151 (2004) A456.
- [21] K. Smith, T. Markel, A. Pesaran, 26th International Battery Seminar & Exhibit, Fort Lauderdale, FL, 2009.
- [22] P. Verma, P. Maire, P. Novák, *Electrochim. Acta* 55 (2010) 6332.
- [23] B.Y. Liaw, E.P. Roth, R.G. Jungst, G. Nagasubramanian, H.L. Case, D.H. Doughty, *J. Power Sources* 119 (2003) 874.
- [24] M. Broussely, P. Biensan, F. Bonhomme, P. Blanchard, S. Herreyre, K. Nechev, R.J. Staniewicz, *J. Power Sources* 146 (2005) 90.
- [25] D. Aurbach, *J. Power Sources* 89 (2000) 206.
- [26] X. Wang, Y. Sone, H. Naito, C. Yamada, G. Segami, K. Kibe, *J. Power Sources* 161 (2006) 594.
- [27] R. Spotnitz, *J. Power Sources* 113 (2003) 72.
- [28] G. Sarre, P. Blanchard, M. Broussely, *J. Power Sources* 127 (2004) 65.
- [29] M. Safari, M. Morcrette, A. Teyssot, C. Delacourt, *J. Electrochem. Soc.* 156 (2009) A145.
- [30] M. Safari, M. Morcrette, A. Teyssot, C. Delacourt, *J. Electrochem. Soc.* 157 (2010) A892.
- [31] S. Santhanagopalan, Q.Z. Guo, P. Ramadass, R.E. White, *J. Power Sources* 156 (2006) 620.
- [32] R.B. Wright, J.P. Christophersen, C.G. Motloch, J.R. Belt, C.D. Ho, V.S. Battaglia, J.A. Barnes, T.Q. Duong, R.A. Sutula, *J. Power Sources* 119 (2003) 865.
- [33] B. Kang, G. Ceder, *Nature* 458 (2009) 190.
- [34] N. Meethong, H.Y.S. Huang, W.C. Carter, Y.M. Chiang, *J. Electrochem. Solid-State Lett.* 10 (2007) A134.
- [35] N. Meethong, H.Y.S. Huang, S.A. Speakman, W.C. Carter, Y.M. Chiang, *Adv. Funct. Mater.* 17 (2007) 1115.
- [36] S.Y. Chung, J.T. Bloking, Y.M. Chiang, *Nat. Mater.* 1 (2002) 123.
- [37] A.K. Padhi, K.S. Nanjundaswamy, J.B. Goodenough, *J. Electrochem. Soc.* 144 (1997) 1188.
- [38] V. Srinivasan, J. Newman, *J. Electrochem. Soc.* 151 (2004) A1517.
- [39] C.S. Wang, U.S. Kasavajjula, P.E. Arce, *J. Phys. Chem. C* 111 (2007) 16656.
- [40] A. Yamada, H. Koizumi, S.I. Nishimura, N. Sonoyama, R. Kanno, M. Yonemura, T. Nakamura, Y. Kobayashi, *Nat. Mater.* 5 (2006) 357.
- [41] I. Bloom, J. Christophersen, K. Gering, *J. Power Sources* 139 (2005) 304.
- [42] I. Bloom, J.P. Christophersen, D.P. Abraham, K.L. Gering, *J. Power Sources* 157 (2006) 537.
- [43] I. Bloom, A.N. Jansen, D.P. Abraham, J. Knuth, S.A. Jones, V.S. Battaglia, G.L. Henriksen, *J. Power Sources* 139 (2005) 295.